ELSEVIER

Polymer 40 (1999) 1961–1967

polymer

A novel laser light-scattering study of enzymatic biodegradation of poly(ε-caprolactone) nanoparticles

Zhihua Gan[a], Jim Tsz Fung[b], Xiabin Jing[a], Chi Wu[b,c,*], W.-K. Kuliche[d]

[a]*Polymer Physics Laboratory, Changchun Institute of Applied Chemistry, Chinese Academy of Sciences, Changchun, Jilin, People's Republic of China*
[b]*Department of Chemistry, The Chinese University of Hong Kong, Shatin, N.T., Hong Kong*
[c]*Department of Chemical Physics, The Open Laboratory of Bond-Selective Chemistry, University of Science and Technology of China, Hefei, Anhui, People's Republic of China*
[d]*Institute of Technical and Macromolecular Chemistry, University Hamburg, Germany*

Received 9 March 1998; revised 22 May 1998; accepted 22 May 1998

Abstract

A successful micronization of water-insoluble poly(ε-caprolactone) (PCL) into narrowly distributed nanoparticles stable in water has not only enabled us to study the enzymatic biodegradation of PCL in water at 25°C by a combination of static and dynamic laser light scattering (LLS), but also to shorten the biodegradation time by a factor of more than 10^3 compared with using a thin PCL film, i.e. a 1 week conventional experiment becomes a 4 min one. The time-average scattering intensity decreased linearly. It was interesting to find that the decrease of the scattering intensity was not accompanied by a decrease of the average size of the PCL nanoparticles, indicating that the enzyme, Lipase Pseudomonas (PS), ''eats'' the PCL nanoparticles one-by-one, so that the biodegradation rate is determined mainly by the enzyme concentration. Moreover, we found that using anionic sodium lauryl sulphate instead of cationic hexadecyltrimethylammonium bromide as surfactant in the micronization can prevent the biodegradation, suggesting that the biodegradation involves two essential steps: the adsorption of slightly negatively charged Lipase PS onto the PCL nanoparticles and the interaction between Lipase PS and PCL.

Keywords: Enzymatic biodegradation; Laser light scattering; PCL nanoparticles

1. Introduction

Biocompatible, biodegradable and non-toxic synthetic aliphatic polyesters, such as poly(ε-caprolactone) (PCL), polylactide and poly(glycolic acid), are very useful in biomedical applications, especially as drug delivery devices [1], because they are completely biodegradable inside the body after its interaction with body fluid, enzyme and cells. The resultant low molar mass molecules in the biodegradation can be either absorbed by the body or removed by metabolism. The biodegradability and stability of synthetic aliphatic polyesters have recently been extensively studied [2–9]. Most of the methods used in these studies are conventional and very time-consuming, such as the total weight loss and oxygen consumption, which lead to macroscopic and rough results. To our knowledge, only a few microscopic and fundamental studies of the biodegradation of synthetic aliphatic polyesters have been reported [10].

For biomedical applications, both in vivo and in vitro studies of the biodegradation of a given polymer are important. Special research interests have been paid to the enzymatic biodegradation [11–15]. Some enzymes, such as extracellular PHB depolymerases, have been used for the study of degradation of poly(hydroxybutyrate), poly(hydroxyvalerate) and PCL, etc. [16–19], and the enzymatic degradation kinetics have also been studied. The Michael–Menten model is a classical enzymatic model [20]. However, this model is usually applied for homogeneous systems in which both enzyme and substrate are water-soluble. Most polymers are water-insoluble, so the enzymatic degradation is a heterogeneous kinetic process [18]. Some investigators have proposed heterogeneous kinetic models. They considered that those enzymes soluble in water first bind to the polymer substrate and then catalyze the hydrolytic scission of polymer chains [21–23]. Previous investigations have indicated that the enzymatic biodegradation happens mainly on the surface because it is difficult for a hydrophilic enzyme to diffuse into a hydrophobic polymer [24]. The chemistry of enzymatic biodegradation of a polyester

* Corresponding author. Tel.: +852-2609-6106; Fax: +852-2603-5057; E-mail: chiwu@cuhk.edu.hk

0032-3861/99/$ - see front matter
PII: S0032-3861(98)00414-5

chain primarily involves the hydrolysis of the polymer chain backbone, much depending on both microscopic and macroscopic properties, such as chemical structure, molar mass, morphology, size and shape of a given polymer sample. The surface area of polymer materials will have a great influence on the enzymatic degradation.

In our laboratory, we have recently developed a range of novel methods for preparing polymer nanoparticles [25,26]. In addition, our previous study has already revealed that Lipase Psuedomonas (PS) was able to accelerate the biodegradation of PCL, and the biodegradation of a macroscopic PCL film with a dimension of $10 \times 10 \times 0.1$ mm^3 could be completed within 1 week in a buffer solution containing 5.0×10^{-4} g ml^{-1} Lipase PS [27]. The micronization of a given polymer sample can greatly increase its surface area. Therefore, a combination of the micronization and enzymatic biodegradation can provide a simple and quick method to evaluate whether a given polymer is biodegradable.

In many studies the turbidimetric method was used to study the degradation of polymer powders or latex suspensions [10,18]. By this method the decrease of light scattering intensity caused by the disappearance of the latex suspension and powders was measured. Compared with this method, laser light scattering (LLS) as a nonintrusive, sensitive and powerful analytical tool and has been widely used to characterize macromolecules and colloids in solution [28]. Using a combination of static and dynamic LLS to monitor the changes of the concentration and hydrodynamic size of polymer nanoparticles under the interaction of an enzyme may lead us to a microscopic picture of the enzymatic biodegradation.

2. Experimental

2.1. Materials

PCL was synthesized by ring-opening polymerization of ε-caprolactone using yttrium trifluoroacetate and triisobutylaluminum $Y(CF_3COO)_3/Al(i\text{-}Bu)_3$ as catalyst [29]. The average molar mass of PCL used in this study was 1.43×10^5 g mol^{-1}. Both cationic hexadecyltrimethylammonium bromide (HTAB) from Eastman Kodak and anionic sodium lauryl sulphate (SDS) from BDH were used as stabilizers in the micronization of PCL without further purification. Lipase PS from *Pseudomonas Cepacia* (courtesy of Amano Pharmaceutical, Japan) was further purified by freeze-drying.

2.2. Micronization of PCL

The PCL nanoparticles were prepared by adding dropwise a dilute PCL acetone solution (2.5×10^{-3} g ml^{-1}) into a large amount of aqueous solution containing either HTAB or SDS as stabilizer, where the stabilizer concentration is higher than its critical micelle concentration (CMC). The acetone and aqueous solutions were constantly mixed by a magnetic stirring during the addition process. When the PCL–acetone solution was added into the aqueous solution, acetone quickly diffused into the water phase because of its good compatibility with water and the hydrophobic PCL chains started to aggregate with each other in water to form nanoparticles which were stabilized by the surfactant molecules absorbed on the particle surfaces. Finally, the acetone, together with a portion of water, was removed under reduced pressure until the mixture reached a desired polymer concentration. Hereafter, the PCL nanoparticles stabilized by HTAB and SDS are respectively denoted as the HTAB-PCL and SDS-PCL nanoparticles.

2.3. LLS

A modified commercial LLS spectrometer (ALV/SP-125) equipped with an ALV-5000 multi-τ digital time correlator and a solid state laser (ADLAS DPY425II, out power of ~400 mW at $\lambda = 532$ nm) was used. The incident beam was vertically polarized with respect to the scattering plane. This spectrometer is capable of measuring both static and dynamic LLS continuously from 6° to 154°. The small angle range from 6° to 20° is particularly useful for the study of large particles.

In static LLS, the angular dependence of the excess absolute time-average scattered intensity, i.e. Rayleigh ratio $R_{vv}(q)$, was measured. For a dilute solution at a relatively small scattering angle θ, $R_{vv}(q)$ can be related to the weight-average molar mass M_w, the second virial coefficient A_2 and the root-mean-square z-average radius $\langle R_g^2 \rangle z^{1/2}$ (or simply as $\langle R_g \rangle$) by [28]

$$\frac{KC}{R_{vv}(q)} \approx \frac{1}{M_w}(1 + \tfrac{1}{3}\langle R_g^2 \rangle_z q^2) + 2A_2C \quad (1)$$

where $K = 4\pi(dn/dc)^2 n^2/(N_A \lambda_0^4)$ and $q = (4\pi n/\lambda_0)\sin(\theta/2)$ with N_A, dn/dc, n and λ_0 being Avogadro's number, the specific refractive index increment, the solvent refractive index, and the wavelength of light in vacuum respectively.

In dynamic LLS, the intensity–intensity time correlation function $G^{(2)}(t, q)$ in the self-beating mode was measured. $G^{(2)}(t, q)$ is related to the normalized electric field time correlation function $g^{(1)}(t, q)$ by Refs. [28,30]

$$G^{(2)}(t, q) = A[1 + \beta |g^{(1)}(t, q)|^2] \quad (2)$$

where A is a measured baseline and $0 < \beta < 1$, depending on spatial coherence of the detection optics. For a polydisperse sample, $g^{(1)}(t, q)$ is related to the line-width distribution $G(\Gamma)$ by Ref. [31]

$$g^{(1)}(t, q) = \int_0^\infty G(\Gamma)\, e^{-\Gamma t}\, d\Gamma \quad (3)$$

$G(\Gamma)$ can be calculated from the Laplace inversion of $G^{(2)}(t, q)$ on the basis of Eqs. (2) and (3). For a pure diffusive relaxation, Γ is related to the translational diffusion coefficient D by $\Gamma/q^2 = D$ at $C \to 0$ and $q \to 0$. In this case, $G(\Gamma)$ can be converted directly to a translational diffusion

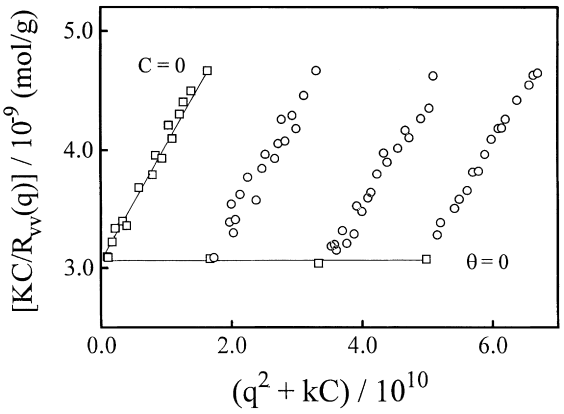

Fig. 1. Typical Zimm plot of the HTAB-PCL nanoparticles in aqueous solution at $T = 25$°C, where C ranges from 2.09×10^{-6} to 6.02×10^{-6} g ml^{-1} and the solutions were clarified with a 0.8 μm filter.

coefficient distribution $G(D)$ or a hydrodynamic radius distribution $f(R_h)$ by using the Stokes–Einstein equation: $R_h = k_B T/(6\pi\eta D)$ with k_B, T and η being the Boltzman constant, the absolute temperature and the solvent viscosity respectively. The detail of LLS instrumentation and theory can be found elsewhere [28,30].

The PCL nanoparticle suspension and the Lipase PS aqueous solution used in LLS were respectively clarified by 0.8 μm and 0.5 μm Millipore filters. In a typical enzymatic biodegradation experiment, a proper amount of the dust-free Lipase PS aqueous solution was added in situ to 2 ml of the dust-free PCL nanoparticle suspension. Both $R_{vv}(q)$ and $G^{(2)}(t, q)$ were measured simultaneously in situ. All the biodegradation experiments were conducted in situ inside the LLS cuvette at $T = 25$°C and $\theta = 15°$, except where stated otherwise.

3. Results and discussion

Fig. 1 shows a typical Zimm plot of the HTAB-PCL nanoparticles in the aqueous solution at 25°C, which incorporates the angular and concentration dependence of the Rayleigh ratio $R_{vv}(q)$ on a single grid. On the basis of Eq. (1), the extrapolation of $[KC/R_{vv}(q)]$ to $C \rightarrow 0$ and $q \rightarrow 0$ leads to M_w and the slopes of $[KC/R_{vv}(q)]_{C \rightarrow 0}$ versus q^2 and $[KC/R_{vv}(q)]_{q \rightarrow 0}$ versus C respectively lead to $\langle R_g \rangle$ and A_2. For the HTAB-PCL nanoparticles, $M_w = 3.31 \times 10^8$ g mol^{-1}, $\langle R_g \rangle = 94.9$ nm and $A_2 \sim 0$; for the SDS-PCL nanoparticles, $M_w = 1.28 \times 10^9$ g mol^{-1}, $\langle R_g \rangle = 135$ nm and $A_2 \sim 0$.

Fig. 2 shows typical time correlation functions of the HTAB-PCL and SDS-PCL nanoparticles in water at 25°C, where $C = 6.25 \times 10^{-6}$ g ml^{-1} and $\theta = 15°$. The inset shows the hydrodynamic radius distributions $f(R_h)$ calculated from the corresponding $G^{(2)}(q, t)$ on the basis of Eqs. (2) and (3) by using a CONTIN Laplace inversion program in the correlator. Both the HTAB-PCL and SDS-PCL nanoparticles are narrowly distributed. The average hydrodynamic radii of $\langle R_h \rangle$, defined as $f(R_h)R_h\,dR_h$, of the HTAB-PCL and SDS-PCL nanoparticles are 103 nm and 153 nm respectively. It is worth noting that both the HTAB-PCL and SDS-PCL nanoparticles were very stable in water and there was no detectable change in $f(R_h)$ even after ~3 months.

Fig. 3 shows the biodegradation time dependence of $[R_{vv}(q)]/[R_{vv}(q)]_o$ of the HTAB-PCL nanoparticles in aqueous solution at 25°C, where $[R_{vv}(q)]_o$ represents the initial Rayleigh ratio before the enzymatic biodegradation. The initial concentrations of the HTAB-PCL nanoparticles and Lipase PS are 6.25×10^{-6} g ml^{-1} and 5.39×10^{-6} g ml^{-1} respectively. The enzyme/polymer ratio is 0.86.

On the basis of Eq. (1), at $q \rightarrow 0$ and $C \rightarrow 0$, $[R_{vv}(q)]/[R_{vv}(q)]_o \propto [CM_w]/[CM_w]_o$. Therefore, the decrease of $[R_{vv}(q)]/[R_{vv}(q)]_o$ could be related to the decrease of either M_w or C, or both. However, the inset in Fig. 3 shows no change in the normalized size distribution, implying no change in the molar mass distribution, so that the decrease of $[R_{vv}(q)]/[R_{vv}(q)]_o$ actually reflects the decrease of the number of the nanoparticles, i.e. the decrease of the relative

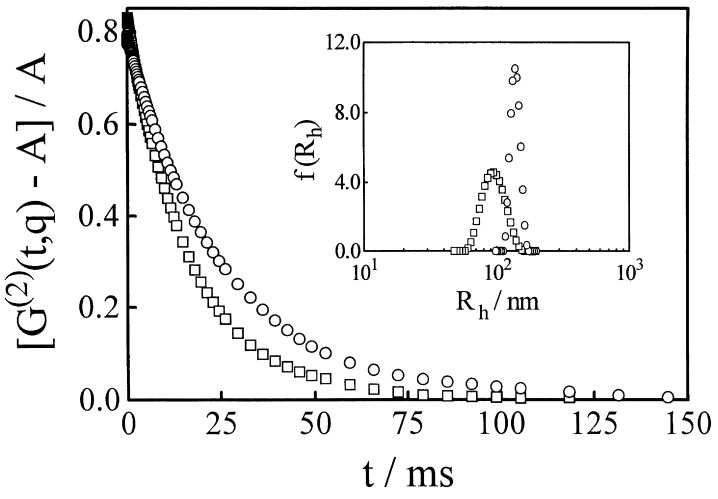

Fig. 2. Typical intensity–intensity time correlation time functions $G^{(2)}(t, q)$ of the HTAB-PCL and SDS-PCL nanoparticles in water at $\theta = 15°$ and $T = 25$°C. The inset shows the corresponding hydrodynamic radius distributions $f(R_h)$: □, HTAB-PCL nanoparticles; ○, SDS-PCL nanoparticles.

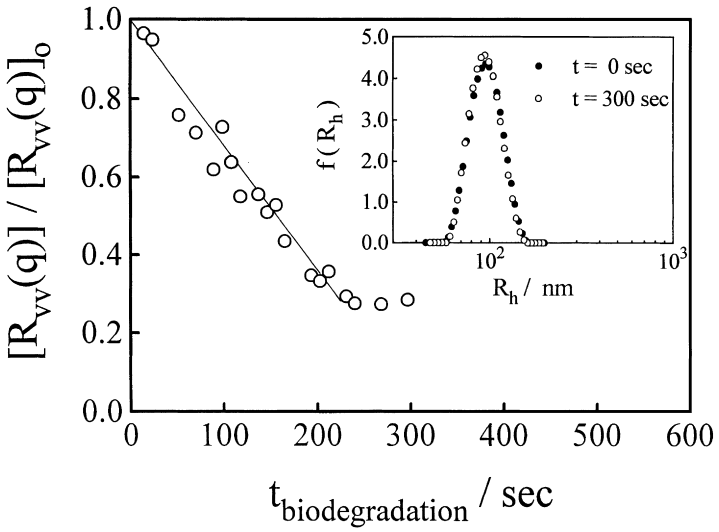

Fig. 3. Biodegradation time dependence of the relative Rayleigh ratio $[R_{vv}(q)]/[R_{vv}(q)]_o$ of the HTAB-PCL nanoparticles in water, where $[R_{vv}(q)]_o$ is the Rayleigh ratio before the biodegradation, $\theta = 15°$ and $T = 25°C$, $C_{o,\,HTAB\text{-}PCL} = 6.25 \times 10^{-6}$ g ml^{-1} and C_o, Lipase PS $= 5.39 \times 10^{-6}$gml^{-1}. The inset shows the corresponding hydrodynamic radius distribution $f(R_h)$ of the HTAB-PCL nanoparticles before the biodegradation and at the end of the biodegradation.

concentration (C/C_o). It is worth noting that, for a similar enzyme/polymer ratio, the weight loss of the HTAB-PCL nanoparticles is more than $\sim 10^3$ times faster than that of a thin PCL film [27], which can be attributed to the huge surface area of the nanoparticles. Therefore, a combination of LLS and micronization has provided a novel and fast method to evaluate the biodegradability of a given polymer.

The solid line in Fig. 3 represents a least squares fitting of $[R_{vv}(q)]/[R_{vv}(q)]_o = 1 - 3.05 \times 10^{-3}t$, revealing that the degradation rate decreases linearly in the enzymatic degradation process. However, it was unexpected to find that the decrease of $[R_{vv}(\theta)]/[R_{vv}(\theta)]_o$ stopped before reaching complete degradation. First, we checked the pH of the suspension, which was 6.3, and found no detectable pH change in the biodegradation process. This forced us to think about why Lipase PS lost its activity in the biodegradation process. It was reported that PCL was ultimately degraded by esterase into 6-hydroxycaproic acid [31]. It is expected that the adsorption of slightly negatively charged Lipase PS to an HTAB-PCL nanoparticle starts the biodegradation of PCL into small water-soluble molecules, which diffuse into water, so that the nanoparticle becomes smaller and smaller and scatters less and less light until all the PCL chains inside this nanoparticle are completely degraded. Then, Lipase PS is surrounded by cationic HTAB surfactant and lose its activity. If our assumption is correct, adding more Lipase PS to the suspension after the biodegradation stops would lead to further biodegradation.

Fig. 4 shows the biodegradation time dependence of $[R_{vv}(q)]/[R_{vv}(q)]_o$ of the HTAB-PCL nanoparticles at 25°C, where the initial enzyme/polymer ratio was 0.015. Clearly, the in situ successive addition of more Lipase PS leads to further degradation. This rules out the possible influence of oxygen because Lipase PS was added into the same solution in the same LLS cuvette and there was no alteration of the oxygen content in the solution. The

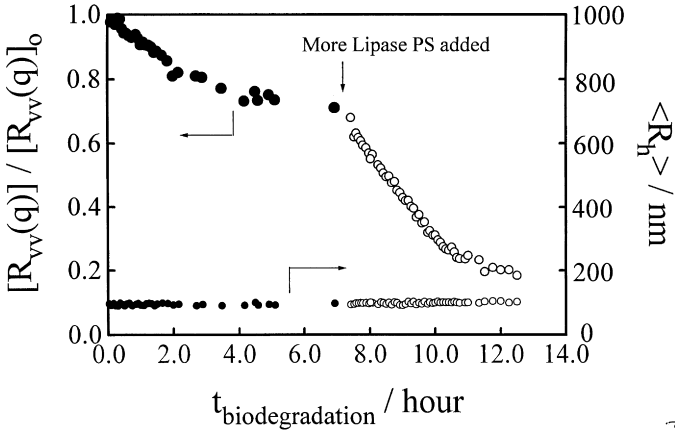

Fig. 4. Biodegradation time dependence of $[R_{vv}(q)]/[R_{vv}(q)]_o$ of the HTAB-PCL nanoparticles after a successive addition of Lipase PS, where $\theta = 15°$, $T = 25°C$, $C_{o,\,HTAB\text{-}PCL} = 8.34 \times 10^{-6}$ g ml^{-1}. In the first stage (●) the Lipase PS concentration was 8.08×10^{-8} g ml^{-1}; in the second stage (○) the Lipase PS concentration was doubled.

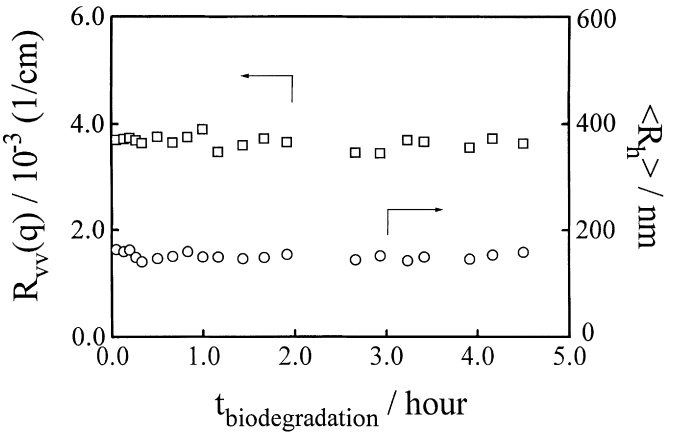

Fig. 5. Biodegradation time dependence of Rayleigh ratio $R_{vv}(q)$ and the average hydrodynamic radius $\langle R_h \rangle$ of the SDS-PCL nanoparticles, where $\theta = 15°$, $T = 25°C$, $C_{o,\ SDS\text{-}PCL} = 6.25 \times 10^{-6}$ g ml^{-1} and $C_{o,\ Lipase\ PS} = 1.36 \times 10^{-6}$ g ml^{-1}.

constant value of $\langle R_h \rangle$ further shows that there is no change of M_w in the biodegradation process. At this point, we can conclude that the cessation of biodegradation after a certain time (shown in Fig. 3) is due to the loss of the enzyme activity. The detail of how Lipase PS lost its bioactivity is still not clear at this time, but is under investigation.

Fig. 5 shows that if anionic SDS, instead of cationic HTAB, was used as the surfactant to stabilize the PCL nanoparticles there was no detectable change in either Rayleigh ratio $R_{vv}(q)$ or $\langle R_h \rangle$, i.e. no enzymatic biodegradation. In order to understand this result, let us examine the nature of Lipase PS. As a protein, Lipase contains many amino-acid groups. In deionized water (pH~6), Lipase PS is slightly negatively charged because its isoelectric point is at pH~5. When the PCL nanoparticle is stabilized by the cationic surfactant HTAB the nanoparticle surface is positively charged, so that Lipase PS can be attracted and adsorbed to the nanoparticles; this results in the occurrence of biodegradation. In contrast, when SDS is used, its anionic nature prevents the adsorption of Lipase PS onto the PCL nanoparticles so that there is no biodegradation. A comparison of Figs 3, and 5 indicates that the adsorption of Lipase PS onto the PCL nanoparticles is the first and essential step of the enzymatic biodegradation.

Figs 6 and 7 respectively show the biodegradation kinetics under different initial polymer and enzyme concentrations, where we have reduced the Lipase PS/PCL ratio to slow down the biodegradation so that we were able to follow it by LLS. In each case, the biodegraded macroscopic weight of PCL W increased nearly linearly in the initial portion, and there is no change in the average size of the PCL nanoparticles because only those PCL nanoparticles remaining can be ''seen'' in dynamic LLS and those that have been biodegraded make no contribution to the

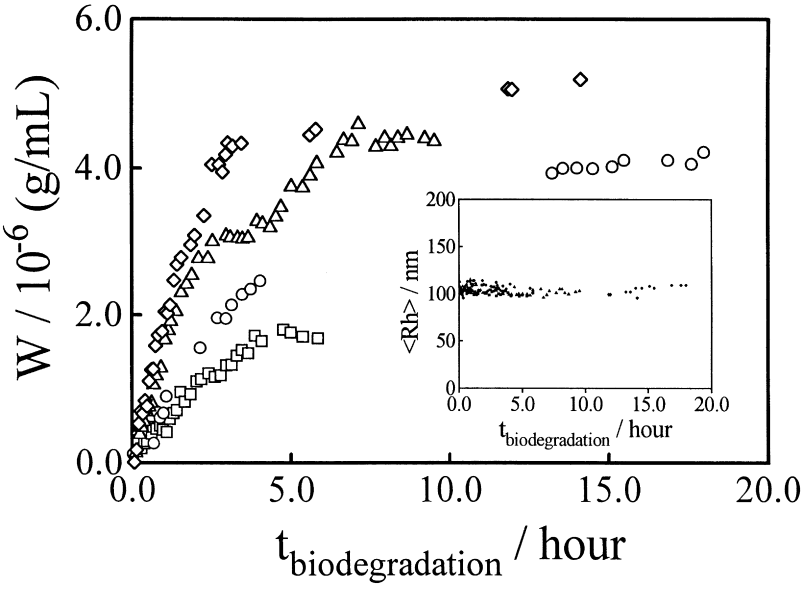

Fig. 6. Enzyme concentration dependence of the biodegradation of the HTAB-PCL nanoparticles, where $\theta = 15°$, $T = 25°C$, $C_{o,\ PCL} = 6.25 \times 10^{-6}$ g ml^{-1}, and $C_{o,\ Lipase\ PS} = 1.33 \times 10^{-8}$ g ml^{-1} (□,■), 2.65×10^{-8} g ml^{-1} (○,●), 5.20×10^{-8} g ml^{-1} (△,▲) and 7.66×10^{-8}gml^{-1}(◇, ◆).

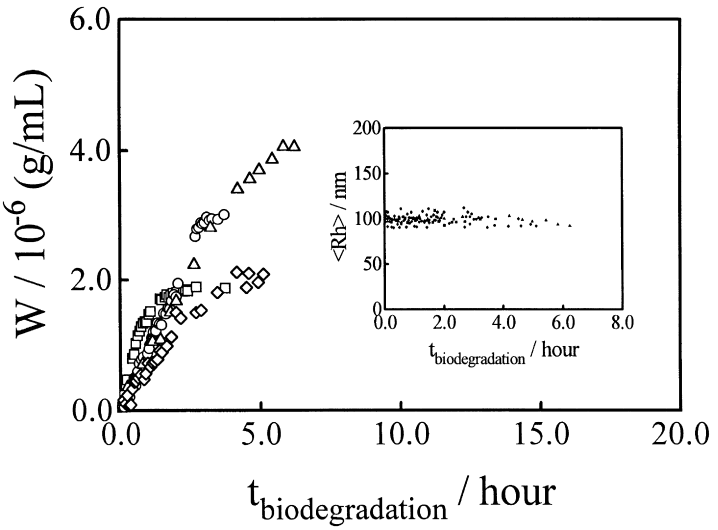

Fig. 7. Polymer concentration dependence of the biodegradation of the HTAB-PCL nanoparticles, where $\theta = 15°$, $T = 25°C$, $C_{o,\ Lipase\ PS} = 7.66 \times 10^{-8}$ g ml^{-1}, and $C_{o,\ PCL} = 2.09 \times 10^{-6}$ g ml^{-1} (□,■), 4.17×10^{-6} g ml^{-1} (○,●); 6.25×10^{-6} g ml^{-1} (△,▲) and 8.23×10^{-6}gml^{-1}(◇, ◆).

scattered light intensity and the average size. The least squares fitting of the initially linear portion of ''W versus t'' leads to the biodegradation rate ν on the basis of $W = \nu t_{biodegradation}$, where ν is the biodegreded polymer weight in the suspension in unit time.

Figs 8 and 9 respectively show the enzyme and polymer concentration dependence of the biodegradation rate ν. For a given amount of PCL, the biodegradation rate increases linearly as the Lipase PS concentration increases and the line in Fig. 8 reprents a least squares fitting of ν/ g ml h$^{-1} = 25.5 C_{o,\ Lipase\ PS}$. On the other hand, for a given amount of Lipase PS, the biodegradation rate remains constant as the PCL concentration increases. As discussed before, the enzymatic biodegradation involves two essential steps: (1) the adsorption of Lipase PS onto the PCL nanoparticles; (2) the interaction between Lipase PS and PCL. In principle, the second step is dependent on the characteristics of Lipase PS and PCL, whereas the first step is related to the total concentration of Lipase PS and PCL. For the Lipase PS–PCL system, the degradation rate will be mainly dependent on the first step. For a given PCL concentration, as shown in Fig. 8, a higher Lipase PS concentration means more Lipase PS molecules can be adsorbed onto PCL nanoparticles. So the total degradation rate increases. However, for a given Lipase PS concentration, the degradation rates are almost uninfluenced by the PCL concentration, as shown in Fig. 9. We have found that the biodegraded macroscopic weight of PCL W increases linearly in the initial portion of enzymatic degradation. This means that the PCL nanoparticles are eaten by Lipase PS one-by-one. So the amount of degradation and the degradation rate of PCL nanoparticles depend only on the concentration of Lipase PS, independent of the PCL concentration. Therefore, the enzymatic degradation rate remains constant at a given Lipase PS concentration but different PCL concentration.

4. Conclusions

We have demonstrated that water-insoluble PCL can be micronized into nanoparticles stable in water at room temperature. Using the PCL nanoparticles instead of a thin PCL film can shorten its biodegradation time by a factor of more than $\sim 10^3$, i.e. a 1 week biodegradation becomes a 4 min process. It has been found that using the cationic surfactant HTAB instead of the anionic surfactant SDS to stabilize the PCL nanoparticles can lead to biodegradation; this is attributed to the fact that Lipase PS is slightly negatively charged. The adsorption of Lipase PS onto the PCL nanoparticles and the interaction between Lipase PS and PCL are two essential steps in the enzymatic biodegradation. The enzymatic biodegradation of the PCL nanoparticles can be effectively monitored by LLS in terms of the excess scattering intensity and the hydrodynamic size. Our results have revealed that the PCL nanoparticles disappear one by one in the course of enzymatic

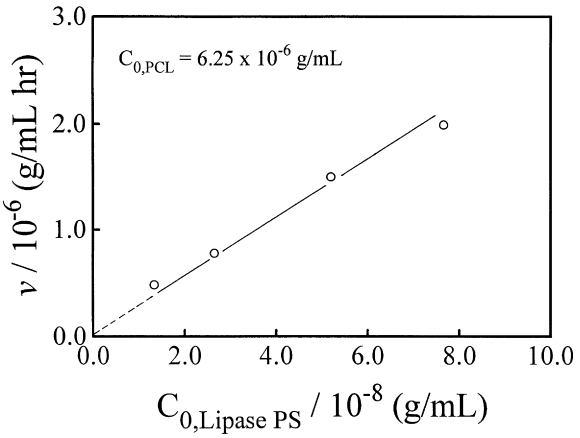

Fig. 8. Lipase PS concentration dependence of the enzymatic biodegradation rate ν of the HTAB-PCL nanoparticles in aqueous solution at $T = 25°C$.

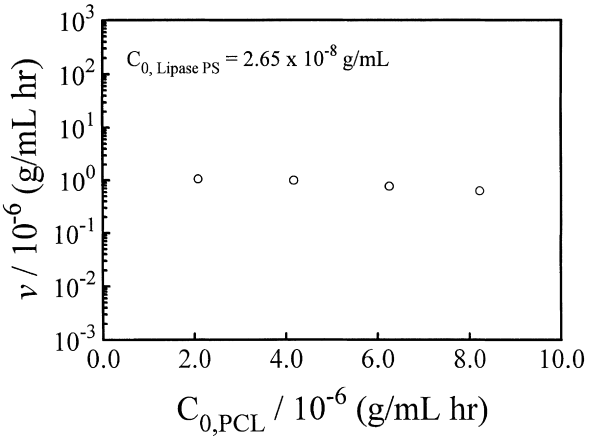

Fig. 9. Polymer concentration dependence of the enzymatic biodegradation rate v of the HTAB-PCL nanoparticles in aqueous solution at $T = 25$°C.

degradation and the biodegradation rate generally increases as the Lipase PS concentration increases. A combination of micronization and LLS not only provides a novel and fast method to evaluate the biodegradability of a given polymer, but also a more reliable and accurate way to study the kinetics of biodegradation.

Acknowledgements

The financial support of the RGC (the Research Grants Council of the Hong Kong Government) Earmarked Grant 1997/98 (CUHK4181/97P, 2160082), The German/Hong Kong Research Fund, and the National Distinguished Young Investigator Fund (1996, A/C No. 29625410) are gratefully acknowledged. Gan and Jing also wish to acknowledge the support of the Science Foundation of Polymer Physics Laboratory, Chinese Academy of Sciences.

References

[1] Mauduit J, Vert M. STP Pharma Sciences 1993;3:197.
[2] Cha Y, Pitt CG. Biomaterials 1990;11:108.
[3] Sawhney AS, Hubbell JA. J Biomed Mater Res 1990;24:1397.
[4] Spenlehauer G, Vert M, Benoit JP, Boddaert A. Biomaterials 1989;10:557.
[5] Park JG. J Controlled Rel 1994;30:161.
[6] Makino K, Arakawa M, Kondo T. Chem Pharm Bull 1985;33:1195.
[7] Coffin MD, McGinity JW. Pharm Res 1992;9:200.
[8] Schmitt EA, Flanagan DR, Linhardt RJ. J Pharm Sci 1993;82:326.
[9] Chacon M, Berges L, Molpeceres J, Aberturas MR, Guzman M. Int J Pharm 1996;141:81.
[10] Lemoine D, Francois C, Kedzierewicz F, Preat V, Hoffman M, Maincent P. Biomaterials 1996;17:2191.
[11] Huang SJ. In: Allen G, Bevington JC, editors. Comprehensive polymer science, chapter 21. Oxford: Pergamon, 1989.
[12] Kaplan DL, Thomas E, editors. Technomic. 1993:1–42.
[13] Lenz R. Adv Polym Sci 1993;107:3.
[14] Swift G. Acc Chem Res 1993;26 :105.
[15] Doi Y. Microbial polyesters. VCH, 1990.
[16] Koyama N, Doi Y. Polymer 1997;38:1589.
[17] Koyama N, Doi Y. Macromolecules 1997;30:286.
[18] Timmins MR, Lenz RW, Fuller RC. Polymer 1997;55:38.
[19] Murphy CA, Anderson JA, Huang SJ. Appl Env Microbiol; 1996; 62:456.
[20] Chang R. Physical chemistry with application to biological systems. New York: Macmillan, 1981.
[21] McLaren AD. Enzymologia 1963;26:237.
[22] Fukui T, Narikawa T, Miwa K, Shirakaru Y, Saito T, Tomita K. Biochem Biophys Acta 1988;952:237.
[23] Mukai K, Yamada K, Doi Y. Int J Biol Macromol 1993;15:361.
[24] Huang SJ, Ho LH, Huang MT, Koenig MF, Cameron JA. In: Doi Y, Fukuda K, editors. Biodegradable plastics and polymers. Amsterdam: Elsevier, 1994:3–7.
[25] Li M, Jiang M, Zhu L, Wu C. Macromolecules 1997;30:2201.
[26] Wu C, Akashi M, Chen M. Macromolecules 1997;30:2187.
[27] Gan ZH, Liang QZ, Jing XB. Polym Degrad Stab 1997;56:209.
[28] Chu B. Laser light scattering, 2nd ed. New York: Academic Press, 1991.
[29] Zhang J, Gan ZH, Jing XB. Polym Int 1998;45:60.
[30] Berne B, Pecora R. Dynamic light scattering. New York: Plenum Press, 1976.
[31] Shirahama H, Yasuda H. In: Doi Y, Fukuda K, editors. Biodegradable plastics and polymers. Amsterdam: Elsevier, 1994:541.